Forced Chemical Mixing in Alloys Driven by Plastic Deformation

S. Odunuga, Y. Li, P. Krasnochtchekov, P. Bellon, and R. S. Averback

Department of Materials Science and Engineering, University of Illinois at Urbana-Champaign, Illinois 61801, USA

(Received 21 March 2005; published 21 July 2005)

Molecular dynamics simulations of forced atomic mixing in crystalline binary alloys during plastic deformation at 100 K are performed. Nearly complete atomic mixing is observed in systems that have a large positive heat mixing and in systems with a large lattice mismatch. Only systems that contained a hard precipitate in a soft matrix do not mix. The amount of mixing is quantified by defining a mean square relative displacement of pairs of atoms, $\sigma^2(R, t)$, that were initially separated by a distance R. Analysis of $\sigma^2(R, t)$ and visual inspection of the displacement fields reveal that forced mixing results from dislocation glide, and that it resembles the forced mixing of a substance advected by a turbulent flow. Consideration of $\sigma^2(R, t)$ also provides a rationalization of compositional self-organization during plastic deformation at higher temperatures.

DOI: 10.1103/PhysRevLett.95.045901 PACS numbers: 66.30.−h, 05.70.Ln, 61.66.Dk, 81.40.Lm

Sustained plastic deformation can force the mixing of chemical elements in crystalline alloys over a wide range of length scales, from the dissolution of nanoscale precipitates in alloys subjected to rolling or fatigue [1,2], to the homogenization of micron-scale tribolayers in frictional wear [3,4], to the macro-scale mixing of Earth's lower and upper mantles [5]. Remarkably, the same mechanism of dislocation glide operates across this entire range of length scales. A decade ago, we noted that this mechanism could force the complete mixing of elements that are immiscible at equilibrium, such as Ag and Cu [6], as long as the deformation takes place at temperatures where thermally activated diffusion processes were suppressed. The stabilization of full solid solutions has indeed been reported after low-temperature, high-energy ball milling in several alloy systems, for example, Ag-Cu [7,8] and Cu-Co [9]. At higher temperatures, where thermal diffusion is no longer frozen, we showed using generic kinetic Monte Carlo simulations that the dynamical competition between forced mixing and thermally activated decomposition leads to the self-organization of the microstructure into compositional patterns [6], and this has now been confirmed experimentally in ball-milled Ag-Cu [10,11].

Some immiscible alloy systems such as Ag-Fe [12] or Ag-Ni [13], however, exhibit very little forced chemical mixing during high-energy ball milling, even at cryogenic temperatures. While this lack of mixing can be simply explained by assuming that the two phases are not co-deformed due to the localization of plastic strain in one of the two phases, several authors have proposed that materials parameters that are related to the *equilibrium* mutual solubility could also account for this behavior [14,15]. In particular, a large lattice mismatch ($\Delta a/a \approx 16\%$ in Ag-Ni) or a large positive heat of mixing ($\Delta H_m =$ 15 kJ/mol in Ag-Ni, 25 kJ/mol in Ag-Fe), have been frequently discussed, but without explanations of why these parameters should be relevant. One might assume that possibly local heating during mechanical working enables atomic diffusion, but very recently, Lund and Schuh [16] have shown that sustained plastic deformation at 0 K, instead of forcing the mixing of alloy components, leads to decomposition or chemical ordering in alloy systems with positive or negative heats of mixing, respectively. These authors employed molecular statics to follow the evolution of two-dimensional Lennard-Jones alloy systems undergoing sustained plastic deformation at 0 K, and thus they avoided any possible local heating. Although the authors proposed that their findings are of general applicability, it remains untested whether similar effects occur in 3D systems as well.

In this Letter we employ molecular dynamics (MD) to simulate the response of model 3D crystalline, binary alloy systems to sustained plastic deformation at low temperature. We show that a large positive heat of mixing and a large lattice mismatch are, in fact, not sufficient to prevent complete mixing. Analysis of the mixing demonstrates that it proceeds by dislocation glide, and we find that this mode of mixing leads to the unusual property in solids that its efficiency increases with the separation distance of atoms. This effect offers a direct rationalization for the dynamical stabilization of compositional patterns during deformation at elevated temperature.

The results presented here concern three model A-B alloys, hereafter referred to as $P1$, $P2$, $P3$, and are based on the Cleri-Rossato Cu and Ag potentials [17]. These are semiempirical, many-body interatomic potentials adjusted for bulk properties, such as elastic constants and lattice parameters. Both elements of the first alloy, $P1$, are taken as Cu, but the cross-terms of the potential are adjusted to yield a very large, positive heat of mixing, 21 kJ/mol at the equiatomic composition. For the $P2$ and $P3$ alloys, Cu and Ag potentials are used for the pure A and B elements, respectively, and thus the lattice mismatch is $\approx 12\%$. The cross-terms in potentials $P2$ and $P3$ are adjusted so that the heat of mixing for $P2$ takes the values of 0.1 and 6.8 kJ/mol for $C_B = 6.3$ and 50 at. %, respectively; and for $P3$ the heats of mixing are 5.7, 15.8, 23.3 and 6.9 kJ/mol for $C_B = 6.3$, 25, 50, and 93.7 at. %, respec-

tively. Four different initial configurations are used to determine their influence on the system response. Configurations with a B precipitate in an A matrix are obtained by starting from a pure A cube containing 32 000 sites on a face centered cubic lattice, thus of edge length ≈ 7.3 nm, and with cube edges along the $\langle 100 \rangle$ directions. A sphere 4.0 nm in diameter is then cut out and replaced by a sphere of B atoms with an equal volume. The B sphere is arbitrarily rotated around two axes to produce an incoherent boundary between the precipitate and the matrix. Atoms with high potential energy are removed progressively until the total energy of the systems stabilizes. All configurations are equilibrated for 5 ps at 100 K before deformation. For run No. 2 the precipitate configuration was relaxed at 500 K for 15 ps, which produced a precipitate with an outer shell having a cube-on-cube orientation relationship with the matrix, and a core containing a twinned tetrahedron.

The MD simulations are performed using periodic boundary conditions and scaling of atomic velocities to maintain a temperature of 100 K [18]. Compressive strains are cyclically applied along the normals of the simulation cell faces by scaling atomic positions at a constant strain rate of 5×10^9 s^{-1}. Such a high strain rate is not a limitation in the present study since we focus on deformation-induced mixing in the low-temperature limit. Each compression lasts 48 ps, thus producing an average strain of 24%.

The amount of mixing is monitored by performing a nearest neighbor analysis and then calculating the same chemical short-range order (CSRO) parameter Ω used by Lund and Schuh [16]. This CSRO parameter takes values of -1.0, 0.0, and 1.0 for microstructures that are fully decomposed, random, or fully ordered, respectively. Figure 1 summarizes the evolution of the CSRO parameters for selected runs. The first observation is that all runs, with the exception of runs No. 1 and No. 4, which are discussed below, tend to a value of Ω near zero, i.e., nearly complete mixing. Contrary to the results reported by Schuh and Lund for 2D systems [16], plastic deformation of an initially random configuration, runs No. 5,6,7,9, never leads to significant decomposition or ordering; $|\Omega|$ remains ≤ 0.1. Starting from decomposed configurations, a large lattice mismatch alone (run No. 3) or a large positive heat of mixing alone (run No. 2) are not sufficient to prevent the nearly full mixing of components. A combination of large lattice mismatch and large positive heat of mixing (run No. 1, run No. 1b) may possibly delay the mixing; notice Ω has not yet reached a steady-state value in run No. 1, but this is more likely due to the particular initial orientation relationship between the precipitate and the matrix, since nearly complete mixing is obtained in run No. lb, which started with a different precipitate-matrix orientation. The only evolution where mixing appears to saturate at a large negative Ω value occurs when a relatively hard precipitate (Cu-like) is embedded in a relatively soft matrix (Ag-like) (run No. 4). We show below that in this case plastic

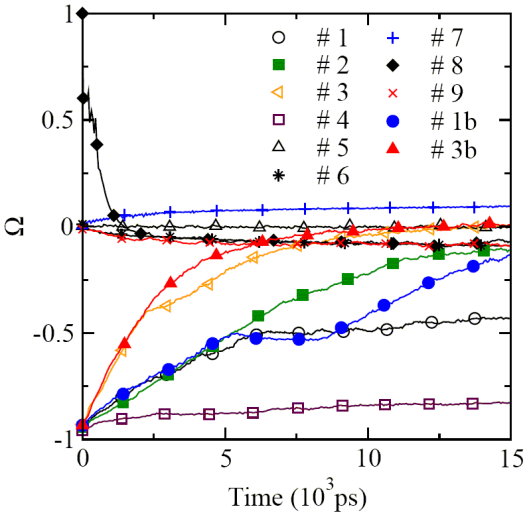

FIG. 1 (color online). Evolution of the chemical short-range order parameter Ω for alloy systems $P1$ (run No. 2), $P2$ (runs No. 3, No. 3b, No. 7), and $P3$ (runs No. 1, No. 1b, No. 4, No. 5, No. 6, No. 8, No. 9). In runs starting at $\Omega \approx -0.95$, the initial configuration is a pure-B single crystal precipitate in a pure-A single crystal matrix ($C_B = 6.4$ at. %), except for run No. 4 where it is a pure-A precipitate in a pure-B matrix. In runs starting at $\Omega = 0$, random configurations are used with $C_B = 50$ at. % (runs No. 6 and No. 7), $C_B = 25$ at. % (run No. 9), and $C_B = 6.3$ at. % (run No. 5). Run No. 8 starts from an $L1_2$ ordered configuration ($C_B = 25$ at. %). Runs No. 1b and No. 3b use the same parameters as in run No. 1 and No. 3, respectively, except for a different initial orientation of the precipitate in the matrix.

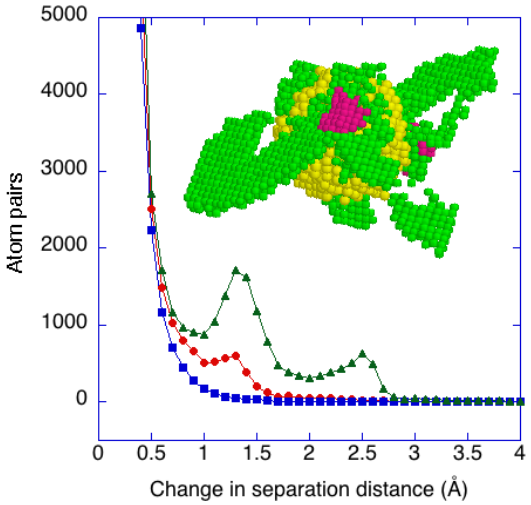

FIG. 2 (color online). Histogram of the change in separation distance of atoms that were first nearest neighbors at $t = 5$ ps, recorded at 6 ps (square), 8 ps (circle) and 15 ps (triangle), for run No. 3. The inset displays, at 8 ps, the B atoms of the precipitate in yellow (light gray), the pairs of atoms belonging to the peak near 1.4 Å in green (gray), and to the peak near 2.5 Å in red (dark gray).

deformation is largely localized in the matrix, thus preventing chemical mixing of the species.

In order to visualize how mixing proceeds, we identify all nearest neighbor pairs of atoms at a certain time, and then recalculate the separation distance of these pairs at later times. For an appropriate initial time and time interval, the histogram of the change of separation distances, Δd, (see Fig. 2) reveals first a peak centered at $\Delta d \approx 1.4$ Å, and then a second peak centered at 2.5 Å. These values correspond to the modulus of the Burgers vectors of $1/6\langle 112\rangle$ partial dislocations and $1/2\langle 110\rangle$ perfect dislocations, respectively. The pairs of atoms belonging to these peaks, as well as the atoms of the precipitate, are illustrated in Fig. 2, using different colors for ease of identification. $\{111\}$ planes sheared by partial and perfect dislocations are clearly revealed. Nanotwins are observed to form by the successive glide of Shockley partials in consecutive $\{111\}$ planes, in agreement with MD simulations performed on nanocrystalline elemental systems [19,20]. By varying the initial time and time interval, this visualization procedure enables a thorough analysis of the initiation, propagation, and transfer of slip. Slip is observed to be initiated by the formation of half loops at the precipitate-matrix interface (Fig. 2), which then expand in the matrix and in the precipitate. Because of the misorientation between the precipitate and the matrix (except for run No. 2), the slip system activated in the precipitate is in general different from the one of the matrix. This leads to the formation of interfacial dislocations, and, in turn, to changes in the relative orientation of the precipitate. In the case of run No. 4, however, slip is mostly confined to the matrix, probably because of the significant difference in shear modulus between the two elements. We thus conclude that in crystalline alloys, a large positive heat of mixing and a large lattice mismatch are not sufficient to prevent forced mixing, and that plastic deformation does not lead to decomposition. The only situation where mixing is suppressed occurs when plastic strain is localized in one of the two species, for instance, due to a difference in shear moduli.

In order to study the mixing efficiency, we calculated the mean square *relative* displacement (MSRD) of pairs of atoms initially separated by a distance R according to the formula

$$\sigma^2(R, t_1, t_2) = \left(\sum_{i=1}^{N} \sum_{j=1}^{z(R,t)} [(R_{ij})_{t2} - (R_{ij})_{t1}]^2 \right) / 2 \sum_{i=1}^{N} z(R, i), \quad (1)$$

where N is the number of atoms in the system, $(R_{ij})_{t1}$ and $(R_{ij})_{t2}$ the vectors joining atoms i and j at times t_1 and t_2, and the summation over j contains all atoms in the cell that are separated from i by a distance $R \pm \delta$ at time t_1; $z(R, i)$ is the number of such atoms. δ is taken here as 0.5 Å. Unlike the more customary mean square displacement of atoms, the time-dependent MSRD enables the identification of the atomic mechanisms of mixing. For example, diffusive mixing yields $\sigma^2 \propto |t_2 - t_1|$, as we show for liquid Cu in Fig. 4 (inset), while laminar flow mixing yields $\sigma^2 \propto |t_2 - t_1|^0$ or $\sigma^2 \propto |t_2 - t_1|^2$ in the case of a velocity field that is either homogeneous or with a gradient. Richardson, moreover, predicted that mixing by turbulent convective flow results in $\sigma^2 \propto |t_2 - t_1|^3$ (see Ref. [21] for a review), in agreement with recent experiments of Ott and Mann [22]. We will return to this point, below.

In order to evaluate the efficiency of the mixing produced by convective flow, it is useful to define *apparent* diffusion coefficients through the relationship $D_{\text{app}} = (1/6)\partial\sigma^2/\partial|t_2 - t_1|$. Figure 3 displays apparent diffusion coefficients obtained from Eq. (1), as a function of R, the separation distance between pairs of atoms, for runs No. 1 and No. 4. The first observation is that the apparent diffusion coefficient *increases* with R. A similar property is observed for the so-called Richardson pairs characterizing the mixing of a substance by a turbulent flow, for which $D \propto R^{4/3}$ [21]. This unusual behavior in solids is in fact fully consistent with mixing forced by the dislocation glide. Indeed, a simple geometric argument indicates that the probability that any dislocation glide plane intersects the line connecting two atoms is proportional to R/L, L being the linear system size. Because of our use of periodic boundary conditions in the simulations, dislocations are mostly generated in pairs. If the separation distance between the pair of dislocations is assumed random, then the probability that two atoms R apart are displaced with respect to one another by the glide of a single pair of dislocations varies as $R(L - R)/L^2$. As seen on Fig. 3, our data fit well to such a functional dependence.

The MSRD defined in Eq. (1) can now be used quite broadly to examine the mechanisms of forced mixing in a variety of situations. For example, if mixing in a particular system proceeds by classical diffusion, which would in-

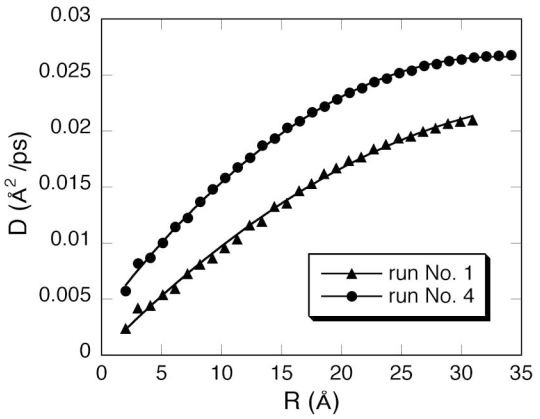

FIG. 3. Apparent diffusion coefficients calculated from Eq. (1) as a function of the separation distance between pairs of atoms, for two runs. The softer matrix in run No. 4 leads to higher D_{app} values. The solid lines are best fit of the data with the functional dependence $R(L - R)$ (see text), with $L = 83.8$ Å in run No. 1 and $L = 65.9$ Å in run No. 4.

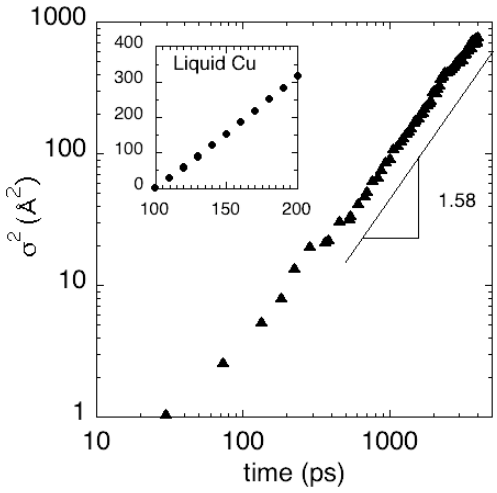

FIG. 4. Evolution of the MSRD, σ^2, with time (run No. 3). Notice the power-law regime with an exponent ≈ 1.58. The initial transient, which is due to interfacial relaxation, represents a small fraction of the MSRD at long times. Inset shows the MSRD calculated for liquid Cu at 1600 K, yielding a linear regime (notice the linear-linear scale) and a diffusion coefficient of 5×10^{-5} cm^2 s^{-1}.

clude the suggestion of injection of interstitials [23], the apparent diffusion coefficients should be independent of R. In the case of grain boundary sliding, [19,20], D_{app} should initially increase with R but then saturate at a value characteristic of the grain size. This method should also offer useful information in the case of amorphous materials, for which the mechanisms of plastic deformation are still debated [24]. For instance, randomly distributed shear-transformation zones (STZs) or flow defects should lead to an apparent diffusion coefficient that is nearly independent of R since these are localized events, while condensation of STZs into shear bands would yield a long-range dependence on R.

Returning to the time dependence of σ^2, we note that if D_{app} depends linearly on R, a simple derivation leads to $\sigma^2 \propto |t_2 - t_1|^n$, with $n = 2$ [25]. This contrasts to the value of $n = 3$ obtained by Richardson for turbulent flow, as noted above. Our data, which are shown in Fig. 4, indeed fit well to a power-law dependence over one decade in time, but with $n \approx 1.5$. The value of n, however, varied with different runs between 1.35 and 1.7, suggesting that the details of the microstructure play a role in the dislocation glide paths.

Finally, the R dependence of the apparent diffusion coefficients provides us with a simple and yet powerful means to rationalize the self-organization of alloys during sustained deformation. Indeed, at temperatures where forced mixing and thermally activated decomposition compete, we can now see why the outcome of this competition is a function of the length scale at which we analyze the materials response. Since forced mixing induced by dislocation activity increases with R, and thermal decomposition is independent of R, one expects the existence of a crossover distance R_c, which provides a good estimate of the scale of the compositional patterns that are stabilized by the deformation.

The research was supported by the U.S. Department of Energy U.S. DOE Basic Energy Sciences, under Grant No. DEFG02-91ER45439 and the U.S. DOE National Nuclear Security Administration, under Grant No. DEFG03-02NA00070 and the U.S. DOE through the University of California under Subgrant B341494, No. 73722. Grants of computer time from the National Center for Supercomputing Applications and the National Energy Research Scientific Computing Center are gratefully acknowledged.

[1] M. Wilhelm and P. Everwin, in *Strength of Alloys and Metals*, edited by P. Haasen (Pergamon, New York, 1979), p. 1089.
[2] M. Sundararaman *et al.*, Acta Metall. Mater. **40**, 1023 (1992).
[3] D. A. Rigney, Wear **245**, 1 (2000).
[4] J. L. Young, Jr., D. Kuhlmann-Wilsdorf, and R. Hull, Wear **246**, 74 (2000).
[5] P. E. van Keken and S. Zhong, Earth Planet. Sci. Lett. **171**, 533 (1999); P. J. Tackley, Science **288**, 2002 (2000); A. K. McNamara, P. E. van Keken, and S.-I. Karato, Nature (London) **416**, 310 (2002).
[6] P. Bellon and R. S. Averback, Phys. Rev. Lett. **74**, 1819 (1995).
[7] T. Klassen, U. Herr, and R. S. Averback, Acta Mater. **45**, 2921 (1997).
[8] F. Delogu *et al.*, Philos. Mag. B **76**, 651 (1997).
[9] C. Gente, M. Oehring, and R. Bormann, Phys. Rev. B **48**, 13244 (1993).
[10] Fang Wu *et al.*, Acta Mater. **49**, 453 (2001).
[11] S. Zghal *et al.*, Acta Mater. **50(19)**, 4711 (2002).
[12] E. Ma, J.-H. He, and P. J. Schilling, Phys. Rev. B **55**, 5542 (1997).
[13] J. Xu *et al.*, J. Appl. Phys. **79**, 3935 (1996).
[14] A. R. Yavari, P. J. Desre, and T. Benameur, Phys. Rev. Lett. **68**, 2235 (1992).
[15] C. Suryanarayana, Prog. Mater. Sci. **46**, 1 (2001).
[16] A. C. Lund and C. A. Schuh, Phys. Rev. Lett. **91**, 235505 (2003); A. C. Lund and C. A. Schuh, J. Appl. Phys. **95**, 4815 (2004).
[17] G. Mazzone *et al.*, Phys. Rev. B **55**, 837 (1997).
[18] H. J. C. Berendsen *et al.*, J. Chem. Phys. **81**, 3684 (1984).
[19] J. Schiotz, F. D. Di Tolla, and K. W. Jacobsen, Nature (London) **391**, 561 (1998).
[20] H. Van Swygenhoven, P. M. Derlet, and A. Hasnaoui, Phys. Rev. B **66**, 024101 (2002).
[21] B. I. Shraiman and E. D. Siggia, Nature (London) **405**, 639 (2000).
[22] S. Ott and J. Mann, J. Fluid Mech. **422**, 207 (2000).
[23] J. Y. Huang *et al.*, J. Mater. Res. **12**, 936 (1997).
[24] See, e.g., F. Spaepen, Acta Metall. **25**, 407 (1977); M. L. Falk and J. S. Langer, Phys. Rev. E **57**, 7192 (1998); J. S. Langer, Phys. Rev. E **70**, 041502 (2004).
[25] S. Odunuga *et al.* (unpublished).